THE JOURNAL OF COMPARATIVE NEUROLOGY 280:553–562 (1989)

Endbulbs of Held and Spherical Bushy Cells in Cats: Morphological Correlates With Physiological Properties

SEISHIRO SENTO AND DAVID K. RYUGO

Department of Anatomy and Cellular Biology, Harvard Medical School, Boston, Massachusetts 02115 (S.S., D.K.R.); Eaton-Peabody Laboratory, Massachusetts Eye and Ear Infirmary, Boston, Massachusetts 02114 (S.S., D.K.R.); Center for Hearing Sciences, Johns Hopkins University School of Medicine, Baltimore, Maryland 21205 (D.K.R.)

ABSTRACT

Single auditory nerve fibers of type I spiral ganglion cells in cats were electrophysiologically characterized by recording with micropipettes inserted into the axon and then labeled by intracellular injections of horseradish peroxidase (HRP) through the same pipettes. This method for staining and studying single neurons allowed us to describe structure-function relationships for labeled endbulbs of Held and the somata of their postsynaptic spherical bushy cells. The silhouette areas of terminal endbulbs and the corresponding somata of spherical bushy cells were determined by planimetry from drawings made with a light microscope and drawing tube. On the presynaptic side, endbulb area is related to fiber characteristic frequency (CF, the frequency to which a fiber is most sensitive) such that the largest endbulbs arise from fibers having CFs between 1 and 4 kHz; smaller endbulbs can arise from fibers of any CF. Endbulb area is not correlated with fiber spontaneous discharge rate (SR). Dividing the endbulb's silhouette area by its silhouette perimeter, however, yields a "form factor" that is a reliable indicator of fiber SR: Endbulbs from fibers of low-medium SR ($\leq$18 spikes/second) have form factor values less than 0.52, whereas endbulbs of high SR fibers (>18 spikes/second) have values greater than 0.52. This form factor should therefore be predictive of SR groupings in auditory fibers for which physiological data are not available.

On the postsynaptic side, the somata of spherical bushy cells receiving endbulbs from low-medium SR fibers are on average smaller than those receiving endbulbs from high SR fibers. In contrast, the nuclei of the spherical bushy cells are the same size regardless of presynaptic fiber SR. Some of the effects of low-medium SR fibers on their postsynaptic targets, when compared to those of high SR fibers, appear to be mimicked by effects of experimentally induced deprivation.

Key words: auditory nerve, cochlear nucleus, hearing, horseradish peroxidase, primary afferents, spontaneous activity

The auditory nerve of mammals contains the axons of two fundamentally distinct populations of ganglion cells (Ryugo et al., '86; Brown et al., '87). Ninety to 95% of the fibers in the nerve are myelinated (Arnesen and Osen, '78) and arise from type I spiral ganglion neurons of the cochlea (Spoendlin, '73). The peripheral processes of these ganglion cells innervate inner hair cells (Kiang et al., '82), and it is these primary neurons for which most information is available (e.g., Kiang, '84). The type I neurons, however, are not a homogeneous population as they can differ across a wide variety of morphological and physiological characteristics

Accepted September 28, 1988.

Dr. Sento's present address is Department of Public Health and Environmental Science, Tokyo Medical and Dental University, 5-45, Yushima, 1-Chome, Bunkyo-ku, Tokyo 113, Japan.

Address reprint requests to Dr. D.K. Ryugo, Johns Hopkins Univ. Sch. of Med., Traylor Research Building, 720 Rutland Avenue, Baltimore, MD 21205.

(e.g., Kiang et al., '65; Liberman, '78, '82; Fekete et al., '84; Rouiller et al., '86; Ryugo and Rouiller, '88).

Spontaneous activity is one fundamental physiological property of the myelinated axons. All-or-none discharges can range from near zero to greater than 100 spikes/second (s/s) and occur in the absence of controlled acoustic stimulation (Walsh et al., '72; Evans, '75). The spontaneous discharge rate (SR) of a fiber is indicative of its sensitivity to sound and its maximum discharge rate (Kiang et al., '65; Liberman, '78; Sachs and Abbas, '74). Moreover, fibers of the different SR groups have distinctive peripheral morphology (Liberman, '82), can be found at all CF values (Kiang et al., '65; Liberman, '78), and systematically differ in their response properties, especially at higher sound levels (Sachs and Young, '79; Young and Sachs, '79; Evans and Palmer, '80; Miller and Sachs, '83, '84; Liberman and Kiang, '84; Costalupes, '85; Rhode and Smith, '85). In this context, fibers of the separate SR groups may have different functional roles in hearing, and if so, may exhibit different connections with neurons in the cochlear nucleus.

In the ventral cochlear nucleus (VCN), type I auditory nerve fibers characteristically give rise to large, axosomatic endings called endbulbs of Held (Held, 1893; Ramón y Cajal, '09; Lorente de Nó, '81). These endbulbs, among the largest synaptic endings in the brain (Lenn and Reese, '66), contact spherical bushy cells (Brawer and Morest, '75; Ryugo and Fekete, '82) and are thought to convey with great fidelity the activity of the presynaptic fiber (e.g., Pfeiffer, '66; Bourk, '76). Spontaneous spike discharges that are recorded from single units of the VCN are wholly dependent on the SR of the auditory nerve (Koerber et al., '66); that is, cutting the auditory nerve essentially abolishes the SR of units in the VCN. In a general way, the SR of an individual spherical bushy cell is inferred to be a rough indicator of the SR of its presynaptic auditory nerve fibers. Given that type I auditory nerve fibers can be segregated into separate functional and morphological groups on the basis of SR, we investigated the extent to which SR differences might be reflected in the structure of endbulbs and their postsynaptic targets.

In the present study, we used intracellular recording and staining methods to analyze individual auditory nerve fibers in cats. The resulting data allowed us to make direct correlations between the fiber's response properties and the morphological features of the endbulb and its postsynaptic neuron. These features have been quantified and found to be reliable indicators of fiber type and spherical cell morphology.

MATERIALS AND METHODS

Physiology and histology

A total of 31 cats, each weighing between 1.4 and 3.7 kg and in good health, were used in this study. Animals were anesthetized with intraperitoneal injections of diallyl barbituric acid in urethane solution (75 mg per kg). Supplemental doses were periodically administered in order to maintain areflexia to paw pinches. The bulla and its bony septum were opened to allow for round window recordings and the external meati were cut just peripheral to the tympanic ring to allow insertion of the acoustic system. The skin and muscle layers of the head were removed so that the skull overlying the posterior fossa could be opened with rongeurs. The dura was reflected over the cerebellum, and the cerebellum was retracted, revealing the auditory nerve between the internal auditory meatus and the cochlear nucleus. Micropipette electrodes were then placed into the nerve under direct visual control.

Upon contacting a unit, a threshold tuning curve and a 15- or 30-second sample of spontaneous activity were obtained before and after the injection of HRP for each unit. The tuning curve was used to determine CF, and SR was defined as spike activity (spikes per second, s/s) in the absence of sound controlled by the experimenter. The ambient acoustic noise within the recording chamber was below the human threshold for hearing even with the ventilation system in operation (Vér et al., '75). Individual fibers were labeled by iontophoresing a 10% solution of HRP (Sigma, type VI) in 0.05 M Tris buffer (pH 7.3) containing 0.15 M KCl through micropipettes bevelled to a final impedance of 40–60 MΩ. Approximately 24 hours after the HRP injections, the cat was given a lethal dose of barbiturate, artificially respirated, and perfused intracardially with buffered fixatives. The perfusion solutions consisted of 50 ml of isotonic saline (37°C) with 0.1% $NaNO_2$, followed immediately by 500 ml of fixative (37°C) containing 0.5% paraformaldehyde, 1.0% glutaraldehyde, and 0.008% $CaCl_2$ in 0.12 M phosphate buffer (pH 7.4), and then 1.5 liters of a second fixative (37°C) containing 1.25% paraformaldehyde, 2.5% glutaraldehyde, and 0.008% $CaCl_2$ in the same buffer solution. Following perfusion and decapitation, the head was immersed in the second fixative (5°C) with enough bone and tissue removed to expose the auditory nerve and cochlear nucleus to the fixative. After 12–24 hours, the brain was removed from the skull and the nerve and nucleus were isolated in a single tissue block. Each block was embedded in gelatin-albumin (Frank et al., '80), sectioned at 40–60-μm thickness with a Vibratome, and kept in serial order. The sections were rinsed several times in 0.1 M Tris buffer (pH 7.6) and then incubated for 1 hour in a solution of 0.5% $CoCl_2$ in Tris buffer. These sections were washed in Tris buffer, washed in 0.1 M phosphate buffer (pH 7.3), and then incubated for 1 hour in a solution of 0.05% 3,3′-diaminobenzidine and 1% dimethylsulfoxide in phosphate buffer (pH 7.3). Sections were washed again and then mounted on glass microscope slides and counterstained with cresyl violet, or postfixed with 0.1% OsO_4 for 15 minutes, stained en bloc with 1% uranyl acetate (overnight), dehydrated, infiltrated with Epon, and flat embedded in a drop of Epon between two sheets (each 25 × 75 mm) of Aclar (Allied Engineered Plastics, Pottsville, PA).

Reconstructions

Only fibers that were well characterized electrophysiologically and recovered with high confidence were used in this analysis. These fibers appeared dark brown or black against the pale-staining tissue of the cochlear nucleus; furthermore, they exhibited distinct swellings at the tips of every terminal branch in the anteroventral cochlear nucleus, thereby providing light microscopic evidence that the ascending branch was completely stained. At the rostral terminus of the ascending branch is typically found a large, axosomatic ending called the endbulb of Held (Ramón y Cajal, '09; Ryugo and Fekete, '82; Fekete et al., '84). Our analysis focused on this large ending and its somatic contact.

"Coded" endbulbs and their postsynaptic spherical cell were drawn with the aid of a light microscope and drawing tube at a total magnification of ×2,000. Because endbulbs are a complex, three-dimensional structure, their parts often overlapped when they were reduced to a planar sil-

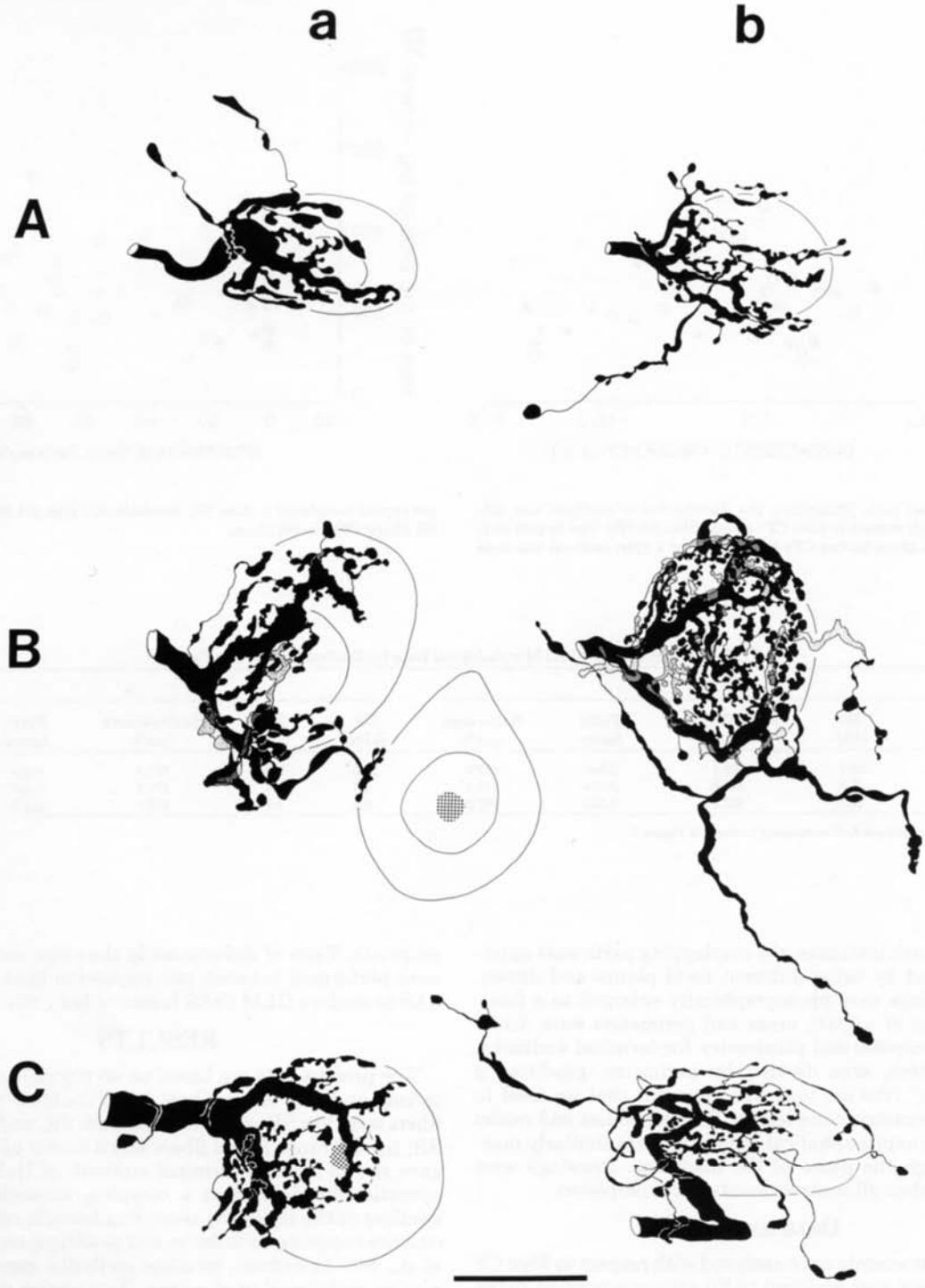

Fig. 1. Drawing tube reconstructions of three pairs of endbulbs of Held (**A–C**). Each pair is from opposite cochlear nuclei of the same cat, representing roughly similar characteristic frequency (CF) ranges but different spontaneous discharge rate (SR) groups. Endbulbs in **column a** are from high SR fibers and those in **column b** are from low-medium SR fibers. Endbulbs in column b have a more "lacy" appearance. See Table 1 for quantitative data on these endbulbs. Scale bar equals 20 μm.

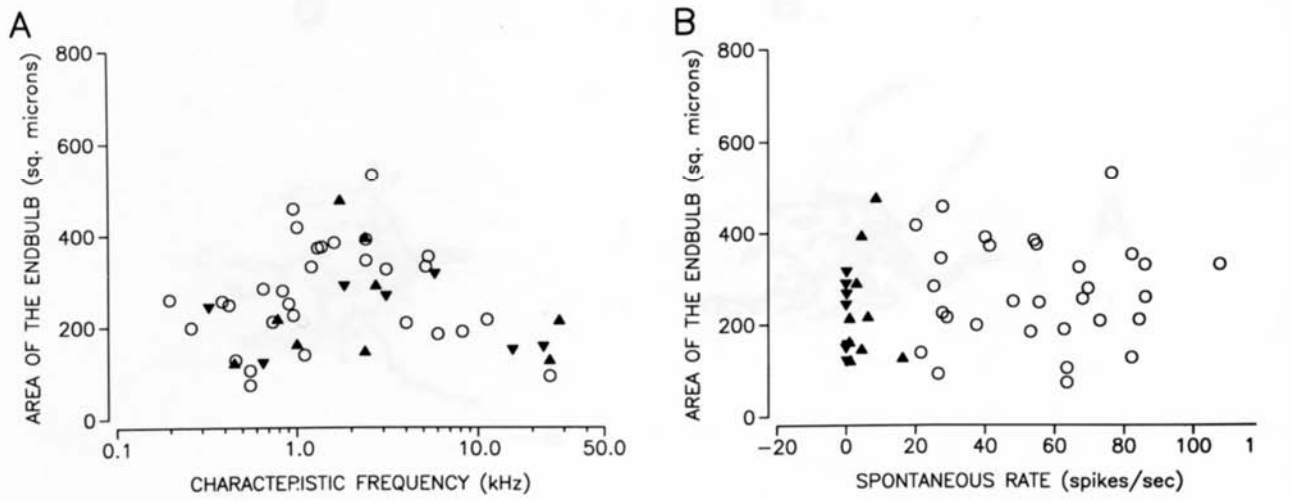

Fig. 2. Scatter plots illustrating the distribution of endbulb size (silhouette area) with respect to fiber CF (**A**) and fiber SR (**B**). The largest endbulbs arise from fibers having CFs between 1 and 4 kHz; endbulb size does not appear correlated to fiber SR. Symbols: (○) high SR fibers; (▲) medium SR fibers; (▼) low SR fibers.

TABLE 1. Physiological and Morphological Data for Endbulbs Shown in Figure 1[1]

	a					b				
	CF (kHz)	SR (s/s)	Endbulb area (μm^2)	Form factor	Soma area (μm^2)	CF (kHz)	SR (s/s)	Endbulb area (μm^2)	Form factor	Soma area (μm^2)
A	8.2	62.7	189.1	0.543	427.0	23.0	0.4	157.3	0.354	395.9
B	2.4	27.3	344.6	0.584	717.1	1.7	8.6	475.2	0.455	533.5
C	0.6	25.3	282.9	0.534	857.2	0.3	0.1	243.1	0.345	431.2

[1]Columns a and b and rows A–C correspond to those in Figure 1.

houette. In such instances, the overlapping parts were optically separated by using different focal planes and drawn. These drawings were photographically enlarged to a final magnification of ×3,000; areas and perimeters were determined by computerized planimetry for terminal endbulbs. The proportion, area divided by perimeter, produced a "form factor" (the μm unit was dropped) that we used to represent geometric complexity. The cell bodies and nuclei of the postsynaptic spherical busy cells were similarly measured through the plane of the nucleolus. Drawings were "decoded" when all measurements were completed.

Data analysis

The measurements were analyzed with respect to fiber CF and SR. Fibers were assigned to SR groups according to the criteria of Liberman, '78: Low SR < 0.5 s/s; medium SR = 0.5–18 s/s; and high SR > 18 s/s. For purposes of statistical comparisons to high SR fibers, low SR fibers and medium SR fibers have been grouped together because they share many electrophysiological and anatomical characteristics. Otherwise, data points for individual fibers are represented by separate symbols in the figures according to their SR. The cytoarchitectonic regions of the cochlear nucleus are used as previously defined (see Fig. 2 of Fekete et al., '84). The means, standard errors of the mean, and Smirnov's P values (nonparametric, two-tailed) are provided where appropriate. Tests of differences in the slope and Y intercept were performed between two regression lines by using the SAS procedure GLM (SAS Institute Inc., '85).

RESULTS

The present data are based on 46 physiologically characterized auditory nerve fibers in 37 cochlear nuclei. Seven fibers were low SR, nine were medium SR, and 30 were high SR; the CF range for all fibers was 0.2–28.2 kHz. Each fiber gave rise to a single terminal endbulb of Held, which was operationally defined as a complex, axosomatic terminal swelling at the tip of the ascending branch, composed of 14 or more components (lobules and swellings; see also Rouiller et al., '86). As defined, terminal endbulbs were easily recognizable and distributed within the anterior division of the AVCN.

Endbulbs of Held

Endbulbs exhibit a wide variety in size and shape. In order to reduce individual variation, pairs of injected fibers were selected so that by using both auditory nerves, they were of similar CF but different SR: Each fiber of one pair was injected in separate nerves, and one cat typically yielded one to three pairs. Examples of some endbulbs stained by this method are illustrated in Figure 1, and a

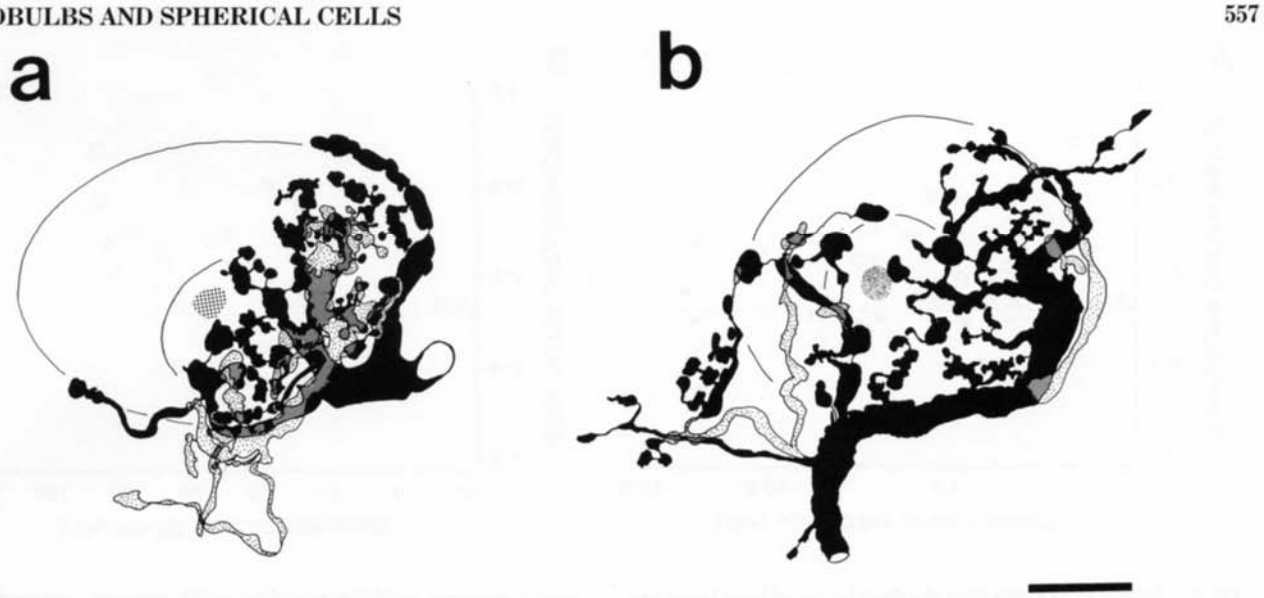

Fig. 3. Drawing tube reconstructions of a pair of terminal endbulbs from the same cat. These drawings illustrate the difficulty in predicting fiber SR on the basis of subjective analysis. **a:** Endbulb in left cochlear nucleus from a fiber having CF = 1.4 kHz, SR = 54.7 spikes/second (s/s), endbulb area = 374.3 μm^2, and form factor = 0.55. **b:** Endbulb in right cochlear nucleus from a fiber having CF = 2.4 kHz, SR = 4.5 s/s, endbulb area = 393.3 μm^2, and form factor = 0.50. Note, however, that the form factor value predicts the fiber's SR group. Scale bar equals 10 μm.

summary of their physiological and morphological measurements is listed in Table 1. Each endbulb consists of a highly branched, cup-shaped arborization that partially encloses the soma of a spherical bushy cell. The parent trunk divides into several thick, knobby branches that in turn generate a number of successively finer branches. The branches of the arborization display irregular varicosities and lobes, many of which are linked together by thin, filamentous processes. Most elements of the endbulb appear in close apposition to the surface of the postsynaptic cell body and form part of the axosomatic embrace. In addition, collateral processes of various lengths and branching patterns are frequently present that distribute en passant and terminal swellings away from the cell body but still to nearby regions (usually within 50 μm). When the swellings are found in neuropil, it is not possible to determine whether they are part of the endbulb contacting distal parts of the same cell (Fig. 1Aa, Ab, Bb, Cb). Sometimes, however, it is clear that they contact a different cell (Fig. 1Ba). The presence or absence, length, or branching patterns of these collaterals do not appear to be related to the fiber's physiological response properties.

Endbulb size. The silhouette area of individual endbulbs was used to represent size. Fiber CF is related to endbulb size (Fig. 2A). As fiber CF increases from 0.2 to approximately 4 kHz, so does the area of the endbulb ($n = 34$, correlation coefficient = 0.48, $P < .01$). As CF continues to increase above 4 kHz, endbulb area decreases ($n = 12$, correlation coefficient = 0.66, $P < .02$). The result is that the largest endbulbs originate from fibers having CFs between 1 and 4 kHz.

The area of the endbulb does not appear to be dramatically related to fiber SR (Fig. 2B). On average (mean ± s.e.m.), there are not statistically significant size differences for endbulbs of the two SR groups; endbulb area for high SR fibers is 271.6 ± 20.1 μm^2, whereas endbulb area for low-medium SR fibers is 230.5 ± 25.1 μm^2 ($P < .10$). These data are not affected by the size variations due to fiber CF (Fig. 2A): For a given CF range, endbulbs of low-medium SR fibers are of equal size compared to those of high SR fibers. Moreover, there is no difference in the areas of endbulbs between low SR fibers and medium SR fibers.

The form factor. The similarity in average size for endbulbs of high SR fibers vs. low-medium SR fibers was unexpected, especially in light of their differences in appearance. That is, the endbulbs of high SR fibers (column a of Fig. 1) seem to have larger but fewer swellings and lobules compared to endbulbs of low-medium SR fibers (column b of Fig. 1). Our subjective impression was that low-medium SR fibers gave rise to lacy, delicate structures, yielding endbulbs that appear to have relatively greater complexity in form. A reliable distinction on the basis of such an impression, however, was often rather difficult to make (Fig. 3).

We used the ratio silhouette area divided by silhouette perimeter to provide an objective value (called the form factor and having no units) for representing each endbulb. This value separated endbulbs into two almost nonoverlapping populations according to SR, regardless of fiber CF or endbulb size (Fig. 4A). The form factor values for endbulbs of high SR fibers (range, 0.46–0.88) were larger than those for endbulbs of low-medium SR fibers (range, 0.34–0.56), and separated endbulbs that appeared morphologically similar (e.g., Fig. 3). There was no systematic relationship between form factor and fiber CF.

Two endbulbs proved to be exceptions to the general rule whereby form factor values could be applied to identify fiber SR. Each endbulb arose from a different cat, yet other endbulbs in these cats followed the rule. It was of interest to note, however, that each exceptional endbulb originated from fibers having "extreme" physiological properties: One endbulb arose from a fiber having the highest SR in our population (107.5 s/s) and the other arose from a fiber having the highest CF (28.16 kHz).

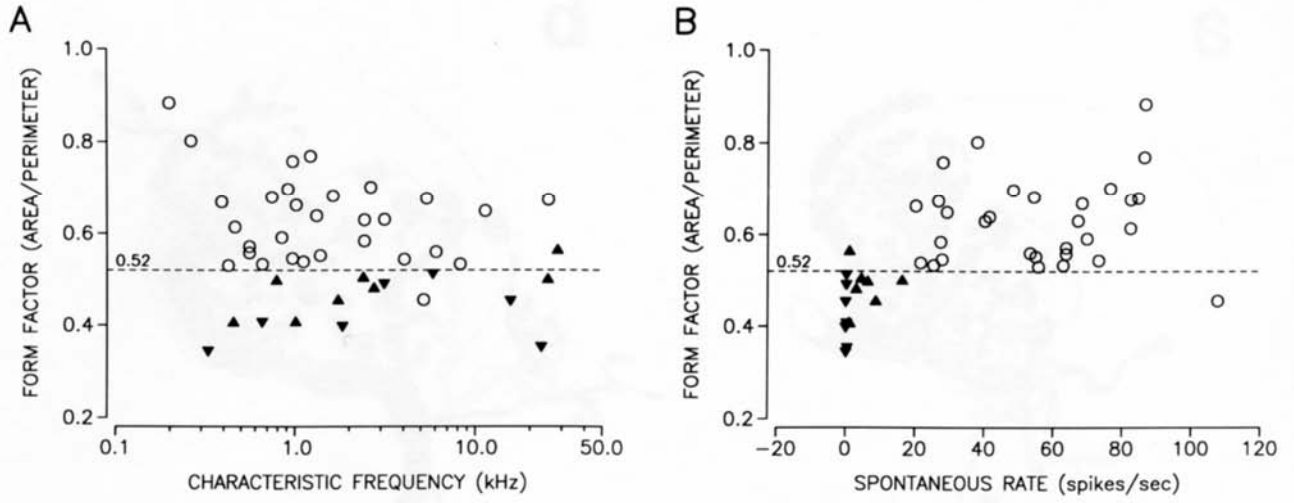

Fig. 4. Scatter plots illustrating the distribution of form factor values (area divided by perimeter, units dropped) of the terminal endbulb with respect to fiber CF (**A**) and fiber SR (**B**). The value, 0.52, almost always separates endbulbs according to SR grouping, irrespective of fiber CF. Symbols: (○) high SR fibers; (▲) medium SR fibers; (▼) low SR fibers.

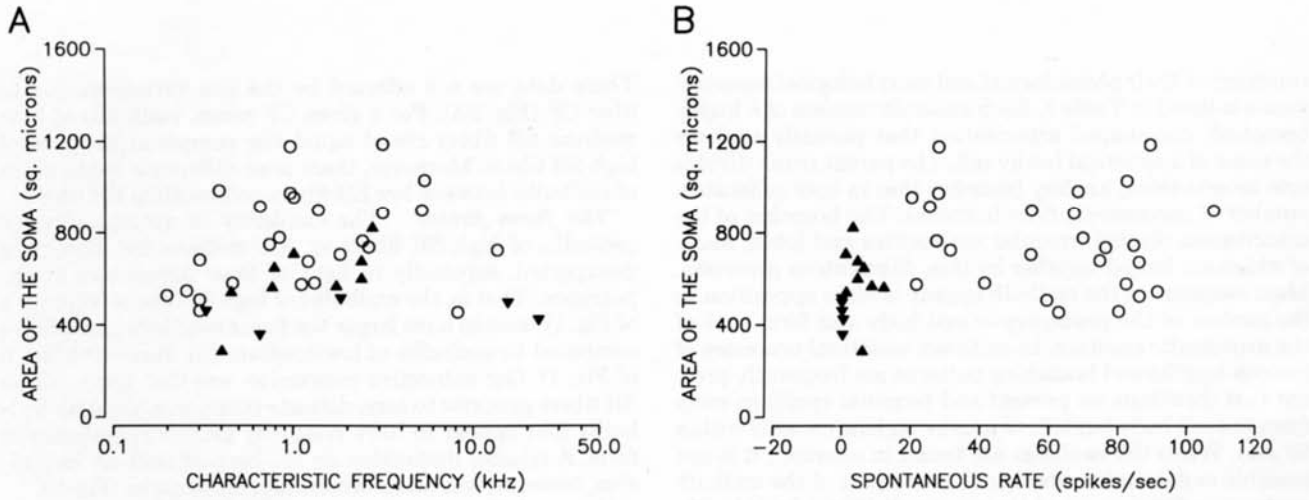

Fig. 5. Scatter plots illustrating the distribution of cell body silhouette area with respect to presynaptic fiber CF (**A**) and SR (**B**). The somata of spherical bushy cells receiving endbulbs from low-medium SR fibers are generally smaller than those receiving endbulbs from high SR fibers. Symbols: (○) high SR fibers; (▲) medium SR fibers; (▼) low SR fibers.

Although the form factor clearly separated endbulbs from fibers having SR above and below 18 s/s, the form factor was not strictly proportional to the SR value across the whole SR range (Fig. 4B). The form factor was more-or-less linearly related to SR from 0 to 40 s/s, but not at higher SR values.

Spherical bushy cells

For the 46 terminal endbulbs of Held in this study, there were 40 cell bodies that could be distinguished within the axosomatic embrace. In those instances where the postsynaptic cell body was not evident, it was because of insufficient counterstaining or because the cell body was separated from the endbulb because of sectioning. Twenty cochlear nuclei were counterstained with cresyl violet and 25 postsynaptic somata were identified as spherical bushy cells on the basis of a prominent perinuclear cap of Nissl material (criterion of Cant and Morest, '79) plus a cytoplasmic "necklace" of Nissl bodies surrounding the nucleus (criterion of Osen, '69). In ten Epon-embedded nuclei, we could observe the outlines of the cell body, nucleus, and nucleolus of 15 additional postsynaptic neurons but could not make cell type identification on the basis of Nissl characteristics. From previous work, however, we have determined that all such cells contacted by labeled endbulbs were indeed spherical bushy cells when examined in the electron microscope (Ryugo and Fekete,

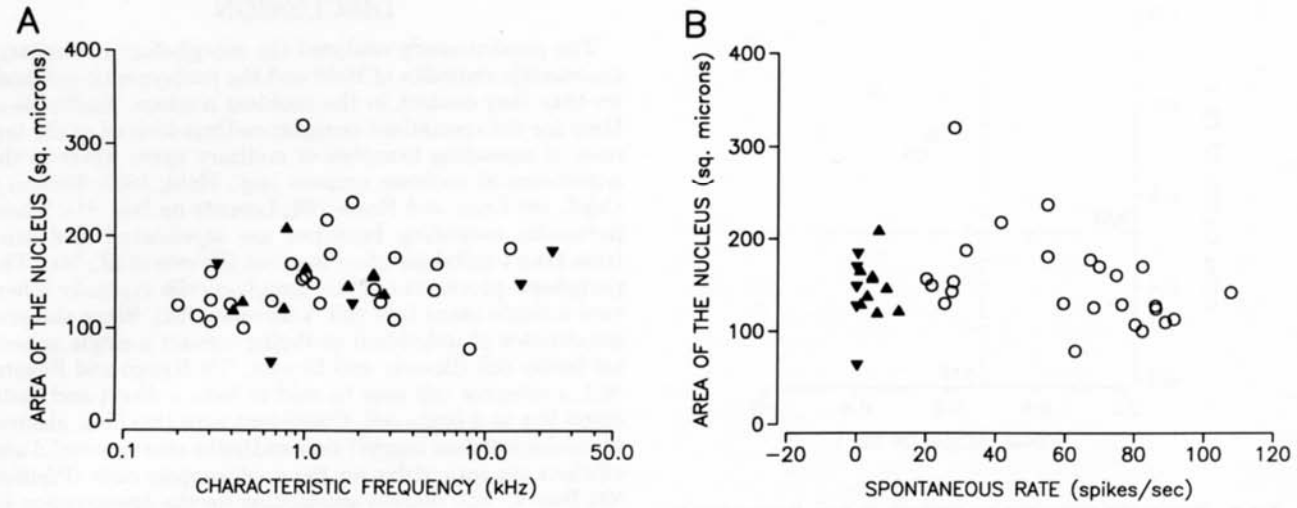

Fig. 6. Scatter plots illustrating the distribution of nuclear silhouette area (of spherical bushy cell) with respect to presynaptic fiber CF (**A**) and fiber SR (**B**). On average, the area of the nucleus is constant. Symbols: (O) high SR fibers; (▲) medium SR fibers; (▼) low SR fibers.

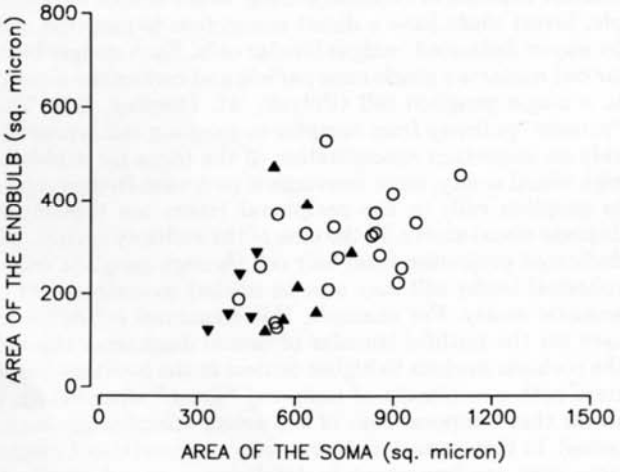

Fig. 7. Scatter plot illustrating the correlation between endbulb size (silhouette area) and its postsynaptic spherical bushy cell size. Symbols: (O) high SR fibers; (▲) medium SR fibers; (▼) low SR fibers.

'82). In addition, although some of the endbulbs of labeled fibers were too faintly stained to be included in the endbulb analysis, the spherical cells they contacted (n = 9) were included because of the high confidence in fiber recovery; this situation resulted in different sample sizes for the endbulb and somatic analyses. It is our working hypothesis that terminal endbulbs contact the somata of spherical bushy cells exclusively in the anterior division of the anteroventral cochlear nucleus.

Cell body size. The silhouette area of spherical bushy cell somata is related to the CF of the fiber giving rise to the presynaptic endbulb (Fig. 5A). For cells postsynaptic to fibers having CFs below 4 kHz, the higher the CF, the larger the silhouette area (n = 34, correlation coefficient = 0.34, $P < .05$). As fiber CF increases above 4 kHz, however, somatic silhouette area decreases (n = 6, correlation coefficient = −0.79, $P < .10$).

The scatter plots illustrate the differences in cell body size between cells postsynaptic to high SR fibers and those postsynaptic to low-medium SR fibers (Fig. 5B). On average, somatic silhouette area of spherical bushy cells postsynaptic to high SR fibers is 719.38 ± 38.2 μm^2 (n = 26) and that of cells postsynaptic to low-medium SR fibers is 522.1 ± 33.4 μm^2 (n = 14). The difference is statistically significant ($P < .01$), but since somatic size is also correlated with presynaptic fiber CF, there is considerable overlap in size distribution (Fig. 5B). Unlike the size distribution of the presynaptic endbulbs (Fig. 2A), at any given CF value, somatic size for cells postsynaptic to low-medium SR fibers is clearly smaller than for those postsynaptic to high SR fibers (Fig. 5A). This relationship between the two SR groups (CF < 4 kHz) is also revealed by similarities in the slopes of their respective regression lines (92.2 for high SR fibers and 104.4 for low-medium SR fibers; SAS, proc. GLM, F = 0.03) and differences in the Y-intercept (612.3 for high SR fibers and 393.5 for low-medium SR fibers; F = 12.21, $P < .002$).

Nuclear size. The area of the nucleus for each spherical bushy cell was taken at the focal plane of the nucleolus. In contrast to somatic size, nucleus size is not correlated with presynaptic fiber CF (Fig. 6A) or fiber SR (Fig. 6B). Average silhouette area of the nucleus is 153.6 ± 9.8 μm^2 for spherical cells postsynaptic to high SR fibers and 145.3 ± 8.9 μm^2 for cells postsynaptic to low-medium SR fibers ($P < .20$).

Endbulbs and spherical bushy cells

Since the silhouette area of endbulbs and postsynaptic cell bodies covaried with respect to fiber CF, it is not surprising that they are correlated to each other (n = 31, corre-

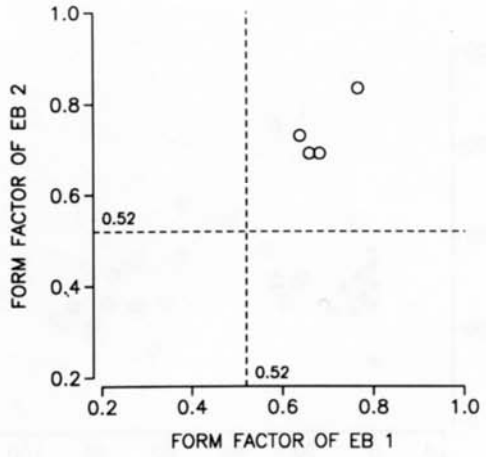

Fig. 8. Scatter plot illustrating the similarity in form factor values for endbulbs converging onto the same spherical bushy cell. For a larger sample size, our prediction is that low-medium SR fibers will have endbulbs whose form factor values place them in the lower left quadrant, whereas high SR fibers will have endbulbs whose form factor values place them in the upper right quadrant.

lation coefficient = 0.49, $P < .01$). That is, the larger spherical cells generally receive the larger endbulbs (Fig. 7). This figure also illustrates that for a given range of somatic areas, there is no systematic difference in the values of presynaptic endbulb areas for high vs. low-medium SR fibers. In contrast, for a given range of endbulb areas, somatic sizes postsynaptic to endbulbs of low-medium SR fibers are on average smaller than those postsynaptic to endbulbs of high SR fibers.

We also analyzed the ratio of endbulb area to somatic area (silhouette area, not actual surface area) in order to investigate whether or not such numbers could indicate the possible number of endbulbs converging upon a single spherical bushy cell. The ratio of endbulb area to somatic area ranged from 0.24 to 0.89. There was no systematic relationship of this ratio for fibers of high vs. low-medium SR, or for fibers of different CFs. Average ratio for high SR fibers is 0.42 ± 0.03 and for low-medium SR fibers is 0.43 ± 0.05.

Endbulbs are reticulated structures, but since the branches of separate endbulbs do not interdigitate, they may be treated as "whole surfaces" within the envelope of the tips of their arborization. Thus, the effective area encompassed by an endbulb can be estimated to be roughly twice what we measured. In addition, if we convert cross-sectional area to surface area, then the somatic area (approximating a sphere) should be multiplied by four, whereas the endbulb area (typically covering a hemisphere) multiplied by two. By these calculations, the conversion factor for both endbulbs and spherical bushy cells is four (and cancels out). On purely numerical grounds, our data imply that two endbulbs should contact a single spherical bushy cell but from one to four endbulbs may do so. These figures are consistent with what has been reported from Golgi studies in young animals (Ramón y Cajal, '09; Lorente de Nó, '81) and HRP material in adults (Ryugo and Fekete, '82).

DISCUSSION

The present study analyzed the morphology of the large axosomatic endbulbs of Held and the postsynaptic cell bodies that they contact in the cochlear nucleus. Endbulbs of Held are the specialized synaptic endings located at the termini of ascending branches of auditory nerve fibers in the anteroventral cochlear nucleus (e.g., Held, 1893; Ramón y Cajal, '09; Lenn and Reese, '66; Lorente de Nó, '81). These particular ascending branches are myelinated and arise from type I spiral ganglion neurons (Fekete et al., '84). The peripheral processes of these ganglion cells typically innervate a single inner hair cell (Liberman, '82). Since the preponderance of individual endbulbs contact a single spherical bushy cell (Brawer and Morest, '75; Ryugo and Fekete, '82), a receptor cell may be said to have a direct and dedicated line to a brain cell. Consistent with this idea, electrophysiological data suggest that endbulbs exert powerful and efficient synaptic drive on the postsynaptic cells (Pfeiffer, '66; Bourk, '76), thereby accounting for the preservation by bushy cells of the discharge patterns conveyed by auditory nerve fibers (Kiang, '75). Thus, single inner hair cells apparently have a dominant, short-latency influence on individual spherical bushy cells across the entire audible frequency range.

The biological significance of such a "one-to-one" relationship between receptor cell and brain cell is of some interest to issues of stimulus coding. In the retina, for example, foveal cones have a direct connection to ganglion cells by way of dedicated, midget bipolar cells. Each midget bipolar cell contacts a single cone pedicle and carries the activity to a single ganglion cell (Polyak, '41; Dowling, '87). This "private" pathway from receptor to ganglion cell is presumably an important specialization of the fovea for achieving high visual acuity, since convergent pathways from receptor to ganglion cells in the peripheral retina are thought to degrade visual acuity. In the case of the auditory system, the dedicated projection from hair cell through ganglion cell to spherical bushy cell may also be related to some aspect of acoustic acuity. For example, this structural substrate allows for the faithful transfer of neural discharges through the cochlear nucleus to higher centers in the auditory brainstem with a minimum of temporal "jitter." Specifically, it seems that temporal cues of the sound stimulus are maintained. In this context, it is generally accepted that binaural time cues are important in localizing a sound source in space, especially when the sound contains low frequencies (e.g., Woodworth and Schlossberg, '38). Consequently, the relationship between inner hair cell, auditory nerve fiber, endbulb, and spherical bushy cell may reflect a specialization for low-frequency sounds. Low-frequency tones elicit phase-locked responses in auditory nerve fibers of all CFs (Rose et al., '67; Kiang and Moxon, '74), and such responses may be one way in which to encode the time of occurrence of a stimulus (e.g., Konishi, '86). The auditory system apparently uses this code for determining time differences related to the time of arrival at the separate ears for a lateralized sound source. Additional neural circuits then presumably convert the time code into a place code necessary for localizing sounds of low-frequency spectra in space (Knudsen et al., '87). Our descriptions of the pathway from inner hair cell to spherical bushy cell are consistent with maintaining a precise temporal representation of binaural, low-frequency sound spectra for the central processor.

Morphological correlates of CF

The present study revealed a relationship between the sizes of terminal endbulbs of Held and postsynaptic spherical bushy cells when fiber CF is below 4 kHz. That is, the largest endbulbs and bushy cells are associated with fibers having CFs between roughly 1 and 4 kHz. This observation confirms and extends a previous report that included both terminal and collateral endbulbs but not postsynaptic cells (Rouiller et al., '86). Although the size data are complicated by SR variations, the size discontinuity at approximately 4 kHz is, nevertheless, consistent with the separation of some physiological properties according to frequency. For instance, saturation rate (Liberman, '78) and phase-locking (Kiang et al., '65; Rose et al., '67; Lavine, '71) differ for units across the 4-kHz reference point, but neither of these features appears related to anything as obvious as the cat's hearing sensitivity as revealed by a behavioral audiogram (Heffner and Heffner, '85). In any case, there is no single parameter that determines somatic size, although it has been proposed that cell body size is related to the extent of the axonal arborization and diameter of the axon (Ramón y Cajal, '09), the size of the target tissue (Voyvodnic, '87), and the neuron's threshold and relative excitability (Henneman et al., '65).

Morphological correlates of SR

Although size differences (silhouette area) between endbulbs of fibers from different SR groups were not observed in our admittedly small sample (see also Ryugo and Rouiller, '88), endbulbs are clearly separated according to SR by their form factor (area/perimeter) values. Because endbulbs are elaborate three-dimensional structures, details regarding their orientation within the tissue section, darkness of staining, and the extent to which different parts superimpose in planar projection could affect the results of the measurements. The impact of these variables was diminished, however, since orientation appeared random, light-staining endbulbs were discarded from the sample, and all endbulbs were "optically sectioned" with the light microscope and drawn so that planar overlap was minimized. Furthermore, analysis was performed "blind" thereby reducing experimenter bias. These considerations and precautions helped to demonstrate that the form factor is a powerful means of predicting fiber SR group, a feature that should be useful in studying labeled endbulbs and auditory nerve fibers whose physiological characterization of SR is not available. Typically, the form factor value for endbulbs of fibers having SR $\leq$ 18 s/s is less than 0.52, whereas that for fibers having SR $>$ 18 s/s is greater than 0.52.

The smaller values imply greater complexity in endbulb shape. The endbulbs of low-medium SR fibers have more but smaller elements when compared to those of high SR fibers; in this way, the endbulb mirrors the features of the ascending branch (Rouiller et al., '86). An obvious question concerns the functional significance of these SR-related differences in endbulb morphology. One idea is that the structural features of endbulbs represent a consequence of general fiber activity. Fibers of the separate SR groups differ in their thresholds to sound and their maximal driven rate (Liberman, '78). Moreover, the sharper tip of the tuning curves of low-medium SR fibers reveals narrower receptive fields. Ultimately, the data imply that low-medium SR fibers should have a lower overall level of activity than high SR fibers in a normal acoustic environment. If such is the case, then the larger components of endbulbs of high SR fibers may be needed to house the greater amount of cellular machinery (e.g., mitochondria, smooth endoplasmic reticulum, vesicles) adjacent to synaptic active zones, or they may reflect activity-related swelling of membranes reported in other neural and secretory systems (Heuser and Reese, '73; Boyne et al., '75; Burwen and Satir, '77).

Interactions between endbulbs and spherical cells

Our data now permit us to address several issues of interest because pre- and postsynaptic elements have been identified and because we have specific information about the activity of the presynaptic neurons. This situation provides us with an excellent opportunity to consider interneuronal phenomena associated with an identified set of central axosomatic synapses. In this context, we wish to discuss our observations with respect to the possible convergence by endbulbs arising from fibers of different SR groupings, because our data argue against such a possibility.

Recall that the somata of spherical bushy cells postsynaptic to endbulbs of low-medium SR fibers are smaller than those postsynaptic to endbulbs of high SR fibers, whereas the nuclei of these spherical bushy cells are relatively uniform in size. In a way, this phenomenon resembles a condition of natural deprivation since it is mimicked by the results of experimental deprivation on somatic and nuclear sizes in several other systems (e.g., Wiesel and Hubel, '63; Benson et al., '84; Moore, '85). The implication is that the level of presynaptic activity determines the size of the postsynaptic cell: A less active neuron (receiving an endbulb from a low SR fiber or being subject to sensory deprivation) would have a smaller cell body than a more active neuron. As a consequence, there should be a segregation of endbulbs onto spherical cells according to fiber SR. On the other hand, if endbulbs of fibers of the different SR groups actually converged onto the same spherical cell, then all such spherical cells should exhibit high SR (and similar general levels of activity) because of an additive effect of the inputs and they should all have cell bodies of similar size. Since this situation is not the case, our indirect data support the SR segregation hypothesis with the proviso that activity levels are correlated to cell body size.

A direct test of this segregation hypothesis would be to record from, inject, and label two auditory nerve fibers connected to the same inner hair cell and having endbulbs that converge onto the same spherical bushy cell. Since the probability of success for such a technical feat is extremely low, an alternative approach is to apply the form factor analysis on endbulbs converging onto the same spherical cell. One method for staining converging endbulbs utilizes large extracellular HRP injections in the auditory nerve. In this way, many fibers are stained, thereby optimizing the chances for visualizing such converging endbulbs. To date, we have four pairs of converging endbulbs whose form factor values are illustrated in Figure 8. The form factor values (range, 0.63–0.83) placed all endbulbs in the high SR group. Moreover, pairs of endbulbs exhibited nearly identical form factor values (range of ratio of FF_1 (small) divided by FF_2 (large), 0.87–0.98). Despite the small sample size, this preliminary evidence also argues for a segregation of endbulb input to spherical bushy cells according to fiber SR group.

ACKNOWLEDGMENTS

The authors gratefully thank M.F. Bourgeois, L.W. Dodds, and D.A. Learson for help with surgery and M.L.

Curby for help with computer programming. We also thank T.E. Benson, P.T. Dunckel, R. Cronin-Schreiber, A.P. Ley, and R.G. Vega for their technical assistance and H. Nitta for advice on statistical analyses. This work was supported by NIH grant NS20156 and NSF grant BNS-8520833.

LITERATURE CITED

Arnesen, A.R., and K.K. Osen (1978) The cochlear nerve in the cat: Topography, cochleotopy, and fiber spectrum. J. Comp. Neurol. *178*:661–678.

Benson, T.W., D.K. Ryugo, and J.W. Hinds (1984) Effects of sensory deprivation on the developing mouse olfactory system: A light and electron microscopic, morphometric analysis. J. Neurosci. *4*:638–653.

Bourk, T.R. (1976) Electrical Responses of Neural Units in the Anteroventral Cochlear Nucleus of the Cat. Ph.D. Dissertation, Massachusetts Institute of Technology, Cambridge, MA.

Boyne, A.F., T.P. Bohan, and T.H. Williams (1975) Changes in cholinergic synaptic vesicle populations and the ultrastructure of the nerve terminal membranes of *narcine brasiliensis* electric organ stimulated to fatigue *in vivo*. J. Cell Biol. *67*:814–825.

Brawer, J.R., and D.K. Morest (1975) Relations between auditory nerve endings and cell types in the cat's anteroventral cochlear nucleus seen with the Golgi method and Nomarski optics. J. Comp. Neurol. *160*:491–506.

Brown, M.C., A.M. Berglund, and D.K. Ryugo (1987) The central projections of type-II spiral ganglion cells in rodents. Soc. Neurosci. Abstr. *13*:1258.

Burwen, S.J., and B.H. Satir (1977) Plasma membrane folds on the mast cell surface and their relationship to secretory activity. J. Cell Biol. *74*:690–697.

Cant, N.B., and D.K. Morest (1979) Organization of the neurons in the anterior division of the anteroventral cochlear nucleus of the cat. Light microscopic observations. Neuroscience *4*:1909–1923.

Costalupes, J.A. (1985) Representation of tones in noise in the responses of auditory nerve fibers in cats. I. Comparisons with detection thresholds. J. Neurosci. *5*:3261–3269.

Dowling, J.E. (1987) The Retina. Cambridge, MA: The Belknap Press of Harvard University Press.

Evans, E.F. (1975) Cochlear nerve and cochlear nucleus. In W.D. Keidel and W.D. Neff (eds): Handbook of Sensory Physiology, Vol. V, Part 2. Berlin: Springer-Verlag, pp. 1–108.

Evans, E.F., and A.R. Palmer (1980) Relationship between the dynamic range of cochlear nerve fibers and their spontaneous activity. Exp. Brain Res. *40*:115–118.

Fekete, D.M., E.M. Rouiller, M.C. Liberman, and D.K. Ryugo (1984) The central projections of intracellularly labeled auditory nerve fibers in cats. J. Comp. Neurol. *229*:432–450.

Frank, E., W.A. Harris, and M.B. Kennedy (1980) Lysophosphatidyl choline facilitates labeling of CNS projections with horseradish peroxidase. J. Neurosci. Methods 2:183–189.

Heffner, R.S., and H.E. Heffner (1985) Hearing range of the domestic cat. Hear. Res. *19*:85–88.

Held, H. (1893) Die centrale Gehorleitung. Arch. Anat. Physiol. Anat. Abt. 201–248.

Henneman, E., G. Somjen, and D.O. Carpenter (1965) Functional significance of cell size in spinal motoneurons. J. Neurophysiol. *28*:560–580.

Heuser, J.E., and T.S. Reese (1973) Evidence for recycling of synaptic vesicle membrane during transmitter release at the frog neuromuscular junction. J. Cell Biol. *57*:315–344.

Kiang, N.Y.S. (1975) Stimulus representation in the discharge pattern of auditory neurons. In D.B. Tower (ed): The Nervous System, Vol. 3, Human Communication and Its Disorders. NY: Raven Press, pp. 81–96.

Kiang, N.Y.S. (1984) Peripheral neural processing of auditory information. In I. Darian-Smith (ed): Handbook of Physiology, Section I, Vol. III, Part 2. Bethesda: American Physiological Society, pp. 639–674.

Kiang, N.Y.S., and E.C. Moxon (1974) Tails of tuning curves of auditory-nerve fibers. J. Acoust. Soc. Am. *55*:620–630.

Kiang, N.Y.S., J.M. Rho, C.C. Northrup, M.C. Liberman, and D.K. Ryugo (1982) Hair-cell innervation by spiral ganglion cells in adult cats. Science *217*:175–177.

Kiang, N.Y.S., T. Watanabe, E.C. Thomas, and L.F. Clark (1965) Discharge Patterns of Single Fibers in the Cat's Auditory Nerve. Cambridge: MIT Press.

Knudsen, E.I., S. du Lac, and S.D. Esterly (1987) Computational maps in the brain. Annu. Rev. Neurosci. *10*:41–65.

Koerber, K.C., R.R. Pfeiffer, W.B. Warr, and N.Y.S. Kiang (1966) Spontaneous spike discharges from single units in the cochlear nucleus after destruction of the cochlea. Exp. Neurol. *16*:119–130.

Konishi, M. (1986) Centrally synthesized maps of sensory space. Trends Neurosci. *9*:163–168.

Lavine, R.A. (1971) Phase-locking in response of single neurons in cochlear nuclear complex of the cat to low-frequency tonal stimuli. J. Neurophysiol. *34*:467–483.

Lenn, N.Y., and T.S. Reese (1966) The fine structure of nerve endings in the nucleus of the trapezoid body and the ventral cochlear nucleus. Am. J. Anat. *118*:375–389.

Liberman, M.C. (1978) Auditory-nerve response from cats raised in a low-noise chamber. J. Acoust. Soc. Am. *63*:442–455.

Liberman, M.C. (1982) Single-neuron labelling in the cat auditory nerve. Science *216*:1239–1241.

Liberman, M.C., and N.Y.S. Kiang (1984) Single-neuron labeling and chronic cochlear pathology. IV. Stereocilia damage and alterations in rate- and phase-level functions. Hear. Res. *16*:75–90.

Lorente de Nó, R. (1981) The Primary Acoustic Nuclei. New York: Raven Press.

Miller, M.I., and M.B. Sachs (1983) Representation of stop consonnants in the discharge patterns of auditory nerve fibers. J. Acoust. Soc. Am. *74*:502–517.

Miller, M.I., and M.B. Sachs (1984) Representation of voice pitch in discharge patterns of auditory nerve fibers. Hear. Res. *14*:257–279.

Moore, D.R. (1985) Postnatal development of the mammalian central auditory system and the neural consequences of auditory deprivation. Acta Otolaryngol. [Suppl.] (Stockh.) *421*:19–30.

Osen, K.K. (1969) Cytoarchitecture of the cochlear nuclei in the cat. J. Comp. Neurol. *136*:453–484.

Pfeiffer, R.R. (1966) Anteroventral cochlear nucleus: Wave forms of extracellularly recorded spike potentials. Science *154*:667–668.

Polyak, S. (1941) The Retina. Chicago, IL: University of Chicago Press.

Ramón y Cajal, S. (1909) Histologie du Système Nerveux de l'Homme et des Vertébrés, Vol. I. Madrid: Instituto Ramón y Cajal (1952 reprint), pp. 754–838.

Rhode, W.S., and P.H. Smith (1985) Characteristics of tone-pip response patterns in relationship to spontaneous rate in cat auditory nerve fibers. Hear. Res. *18*:159–168.

Rose, J.E., J.F. Brugge, D.J. Anderson, and J.E. Hind (1967) Phase-locked response to low-frequency tones in single auditory nerve fibers of the squirrel monkey. J. Neurophysiol. *30*:769–793.

Rouiller, E.M., R. Cronin-Schreiber, D.M. Fekete, and D.K. Ryugo (1986) The central projections of intracellularly labeled auditory nerve fibers: An analysis of terminal morphology. J. Comp. Neurol. *249*:261–278.

Ryugo, D.K., L.W. Dodds, and N.Y.S. Kiang (1986) Axon morphology of type II spiral ganglion cells in cats. Soc. Neurosci. Abstr. *12*:779.

Ryugo, D.K., and D.M. Fekete (1982) Morphology of primary axosomatic endings in the anteroventral cochlear nucleus of the cat: A study of the endbulbs of Held. J. Comp. Neurol. *210*:239–257.

Ryugo, D.K., and E.M. Rouiller (1988) The central projections of intracellularly labeled auditory nerve fibers in cats: Morphometric correlations with physiological properties. J. Comp. Neurol. *271*:130–142.

Sachs, M.B., and P.J. Abbas (1974) Rate versus level functions for auditory-nerve fibers in cats: Tone-burst stimulation. J. Acoust. Soc. Am. *56*:1835–1847.

Sachs, M.B., and E.D. Young (1979) Encoding of steady-state vowels in the auditory nerve: Representation in terms of discharge rate. J. Acoust. Soc. Am. *66*:470–479.

SAS Institute Inc. (1985) SAS User's Guide: Statistics, 5th Edition. Cary, NC: SAS Institute Inc.

Spoendlin, H. (1973) The innervation of the cochlear receptor. In A.R. Moller (ed): Basic Mechanisms in Hearing. NY: Academic Press, pp. 185–234.

Vér, I.L., R.M. Brown, and N.Y.S. Kiang (1975) Low-noise chambers for auditory research. J. Acoust. Soc. Am. *58*:392–398.

Voyvodnic, J.T. (1987) Dendritic geometry of sympathetic ganglion cells is regulated by postganglionic target size. Soc. Neurosci. Abstr. *13*:574.

Walsh, B.T., J.B. Miller, R.R. Gacek, and N.Y.S. Kiang (1972) Spontaneous activity in the eighth cranial nerve of the cat. Int. J. Neurosci. *3*:221–236.

Wiesel, T.N., and D.H. Hubel (1963) Effects of visual deprivation on morphology and physiology of cells in the cat's lateral geniculate body. J. Neurophysiol. *26*:978–993.

Woodworth, R.S., and H. Schlossberg (1938) Experimental Psychology. NY: H. Holt and Reinhart Press.

Young, E.D., and M.B. Sachs (1979) Representation of steady-state vowels in the temporal aspects of the discharge patterns of populations of auditory-nerve fibers. J. Acoust. Soc. Am. *66*:1381–1403.